LATEST RESEARCH & DEVELOPMENT IN THERMODYNAMIC CYCLES AND HEAT TRANSFER IN NUCLEAR AND THERMAL POWER INDUSTRIES

Pioro* I.L., Popov R. and Mahdi M.
*Author for correspondence
Faculty of Energy Systems and Nuclear Science
University of Ontario Institute of Technology
2000 Simcoe Street North, Oshawa, ON L1H 7K4
Canada
E-mail: Igor.Pioro@uoit.ca

ABSTRACT

It is well known that electrical-power generation is the key factor for advances in industry, agriculture, technology and the level of living. Also, strong power industry with diverse energy sources is very important for country independence. In general, electrical energy can be generated from: 1) burning mined and refined energy sources such as coal (40%), natural gas (23%), oil (4%), and nuclear (11%); and 2) harnessing energy sources such as hydro (17%), and biomass, wind, geothermal, solar, and wave power (all together about (5%).

Today, the main sources for electrical-energy generation are: 1) thermal power – primarily using coal and secondarily - natural gas; 2) "large" hydro power; and 3) nuclear power from various reactor designs. The balance of the energy sources is from using oil, biomass, wind, geothermal and solar, and have visible impact just in some countries.

The driving force in the power industry is thermal efficiency or just efficiency for some energy sources. Modern power plants have the following gross thermal efficiencies: Combined-cycle power plants up to 62%; supercritical-pressure thermal power plants – up to 55%; subcritical-pressure thermal power plants – up to 43%; carbon-dioxide-cooled and sodium-cooled reactors Nuclear Power Plants (NPPs) – up to 40 and 42%, respectively; and water-cooled reactors NPPs – 30–36% only. According to the thermodynamics higher thermal efficiencies correspond to higher temperatures / pressures. Therefore, the paper presents the current status of power plants and latest R&D in thermodynamic cycles and heat transfer in nuclear- and thermal-power industries.

1. ELECTRICITY GENERATION IN THE WORLD

It is well known that electric-power generation and usage is the key factor for advances in industry, agriculture and the socio-economic level of living (see Table 1 and Fig. 1) [1, 2]. Also, strong power industry with diverse energy sources is very important for a country's independence. In general, electrical energy (see Figs. 2 and 3) can be generated from: 1) burning mined and refined energy sources such as coal, natural gas, oil, and nuclear; and 2) harnessing energy sources such as hydro, biomass, wind, geothermal, solar, and wave power.

Today, the main sources for global electrical-energy generation are: 1) Thermal power - primarily using coal (39.9%) and secondarily - natural gas (22.6%); 2) "Large" hydro power (17.2%); and 3) Nuclear power from various reactor designs (11.2%). The remaining 9.2% of the electrical energy is generated using oil (4.2%) and the rest 5% - with biomass, wind, geothermal, and solar energy in selected countries (see Figs. 2 and 3). In addition, energy sources, such as wind and solar (see Fig. 4) and some others, like wave-power, are intermittent from depending on Mother Nature.

Table 2 lists 11 top largest power plants of the world, and Table 3 - the largest power plants of the world by energy source.

It should be noted that the following two parameters are important characteristics of any power plant: 1) Overall (gross) or net efficiency[1] of a plant; and 2) Capacity factor[2] of a plant. Power-plant efficiencies are listed in Table 4a for modern thermal power plants and in Table 4b – for current NPPs, and average capacity factors of power plants – in Tables 2 and 5.
Usually, thermal power plants operate semi-continuously, because of a high operating costs (mainly, high prices of fuel) and relatively low capital costs. Also, thermal and hydro power plants have to cover daily and seasonal energy consumption variations including unpredictable variations in electricity generation from wind and solar power plants (if an energy grid contains them) (for details, see Fig. 4). On opposite, Nuclear Power Plants (NPPs) operate continuously at the maximum installed capacity due to relatively low operating costs.

The relative costs of electrical energy generated by any system are not only dependent on construction capital costs and operating expenses, but also dependent on the capacity factor. The higher the capacity factor the better, as generating costs fall proportionally. However, some renewable-energy sources with exception of large hydro-electric power plants can have

[1] Gross efficiency of a unit during a given period of time is the ratio of the gross electrical energy generated by a unit to the energy consumed during the same period by the same unit. The difference between gross and net efficiencies is internal needs for electrical energy of a power plant, which might be not so small (5% or even more).

[2] The net capacity factor of a power plant is the ratio of the actual output of a power plant over a period of time (usually, during a year) and its potential output if it had operated at full nameplate capacity the entire time. To calculate the capacity factor, the total amount of energy a plant produced during a period of time should be divided by the amount of energy the plant would have produced at the full capacity. Capacity factors vary significantly depending on the type of a plant. Unfortunately, this important factor is quite seldom listed in many sources!

significantly lower capacity factors compared to those of thermal- and nuclear-power plants (see Tables 2 and 5).

Consequently, in today's politico-socio-economic world, many governments subsidize selected low capacity-factor sources, like wind and solar, using preferential rates, enforced portfolios, artificial tariffs, market rules, and power-purchase agreements to partly offset the competitive advantage of lower cost generation from natural gas, coal and nuclear. It is against the market background, of low cost natural gas and of directly or indirectly subsidized alternates, that today's and tomorrow's NPPs must operate.

An example of how various energy sources generate electricity in a grid can be illustrated based on the Province of Ontario (Canada) system. Currently, the Province of Ontario (Canada) has completely eliminated coal-fired power plants from the electrical grid. Some of them were closed, others – converted to natural gas. Figure 3a shows installed capacity and Fig. 3b – electricity generation by energy source in the Province of Ontario (Canada) in 2015. Analysis of Fig. 3a shows that in Ontario major installed capacities in 2015 were nuclear (38%), gas (29%), hydro (25%), and renewables (mainly wind) (8%). However, electricity (see Fig. 3b) was mainly generated by nuclear (60%), hydro (24%), natural gas (8.7%), and renewables (mainly wind) (4.9%).

Figure 4a,b shows power generated by various energy sources in Ontario (Canada) on June 17, 2015 (a) and corresponding to that capacity factors of various energy sources (b). Analysis of Fig. 4 shows that electricity that day from midnight till 3 o'clock in the morning was mainly generated by nuclear, hydro, gas, wind, and biofuel. After 3 o'clock, biofuel power plants increased slightly electricity generation followed by hydro and gas-fired power plants. Also, at the same time, wind power plants started to generate slightly more electricity due to Mother Nature. However, after 7 o-clock wind power started to fluctuate and, eventually, decreased quite significantly. After 6 o'clock in the morning, solar-power plants started to generate some electricity. During a day, hydro, gas-fired and biofuel power plants had variable electricity generation to compensate changes in consumption of electrical energy and variations in generating electricity with wind and solar power plants. After 9 o'clock in the evening, energy consumption started to drop in the province, and at the same time, wind power increased by Mother Nature. Therefore, gas-fired, hydro and biofuel power plants decreased energy generation accordingly. It should be noted that, usually, NPPs operate at about 100% of installed capacity providing reliable basic power to the grid.

Table 1 Electrical-Energy Consumption (EEC) per capita in selected countries (listed here just for reference purposes) [1] (Data for all countries in the world are listed in [1])

No	**Country**	**Population in millions (July 2015)**	**Electrical Energy Consumption (EEC)**		**HDI (2014)**		**Explanations to Table**
			TWh (2012-2014)	**W/Capita**	**Rank**	**Value**	
1	Norway	5.21	120.5	2,618	1	0.944	* EEC, $\frac{\text{W}}{\text{Capita}} = \frac{\left(EEC,\ \frac{TW\,h}{year}\right) \times \frac{10^{12}}{365\text{ days} \times 24\text{ h}}}{(\text{Population, Millions}) \times 10^{6}}$. ** HDI – Human Development Index by United Nations (UN); HDI is a comparative measure of life expectancy, literacy, education and standards of living for countries worldwide. HDI is calculated by the following formula: HDI= $\sqrt[3]{\text{LEI}\times\text{EI}\times\text{II}}$, where LEI - Life Expectancy Index, EI - Education Index, and II - Income Index. It is used to distinguish whether the country is a developed, a developing or an under-developed country, and also to measure the impact of economic policies on quality of life. Countries fall into four broad human-development categories, each of which comprises ~42 countries: 1) Very high – 42 countries; 2) high – 43; 3) medium – 42; and 4) low – 42.
2	Germany	80.85	540.1	762	6	0.916	
3	USA	321.37	3,832.0	1,360	8	0.915	
4	Canada	35.10	524.8	1,706	9	0.913	
5	UK	64.09	319.1	568	14	0.907	
6	Japan	126.92	921.0	828	20	0.891	
7	Italy	61.86	303.1	559	27	0.873	
8	France	66.55	451.1	773	22	0.888	
9	Russia	142.42	1,037.0	831	50	0.798	
10	Brazil	204.26	483.5	270	75	0.755	
11	Ukraine	44.43	159.8	410	81	0.747	
12	China	1,367.49	5,523.0	461	90	0.727	
13	World	7,256.49	19,710.0	310	103	0.711	
14	India	1,251.70	864.7	79	130	0.609	
15	Afghanistan	32.56	3.9	14	171	0.465	
16	Chad	11.63	0.2	2	185	0.392	
17	Niger	18.05	0.9	6	188	0.348	

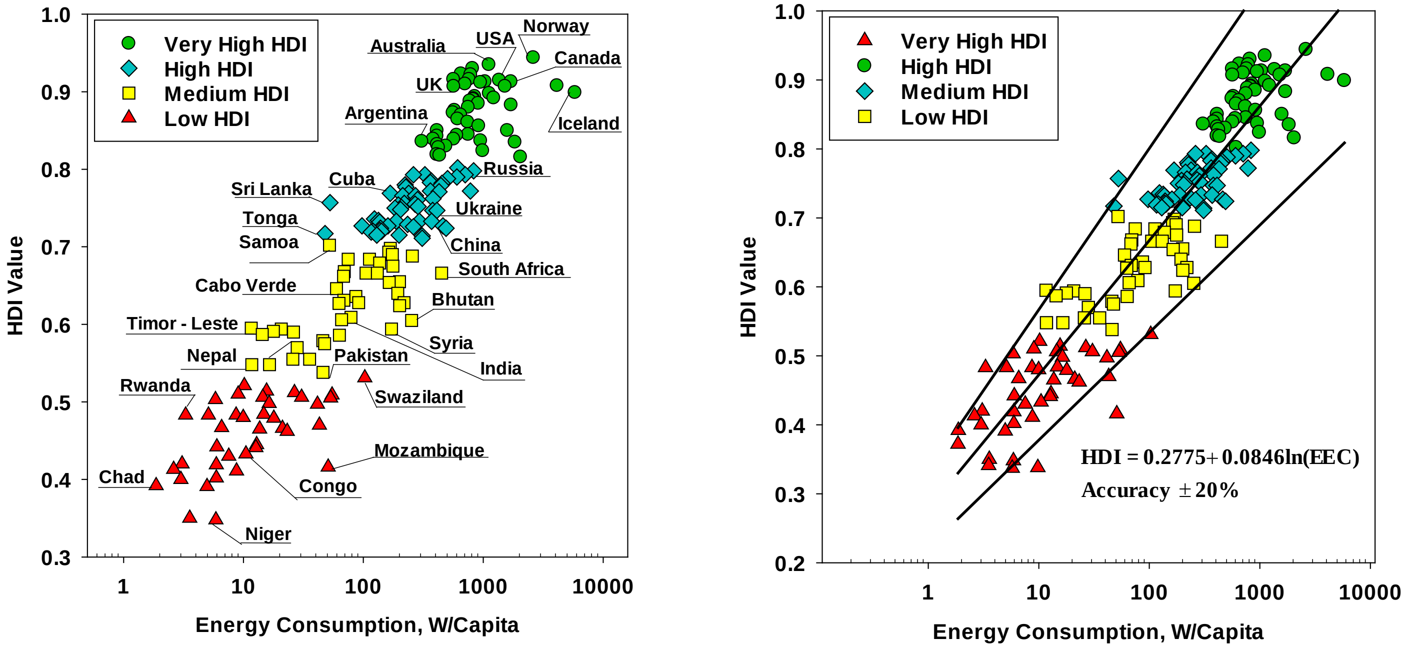

(a) (b)

Figure 1 Effect of Electrical-Energy Consumption (EEC) on Human Development Index (HDI) for all countries of the world (based on data from United Nations (2016) and The World Fact Book (2013)): (a) graph with selected countries shown and (b) HDI correlation (in general, the HDI correlation might be an exponential rise to maximum (1), but based on the current data it is a straight line in regular – logarithmic coordinates) [1]

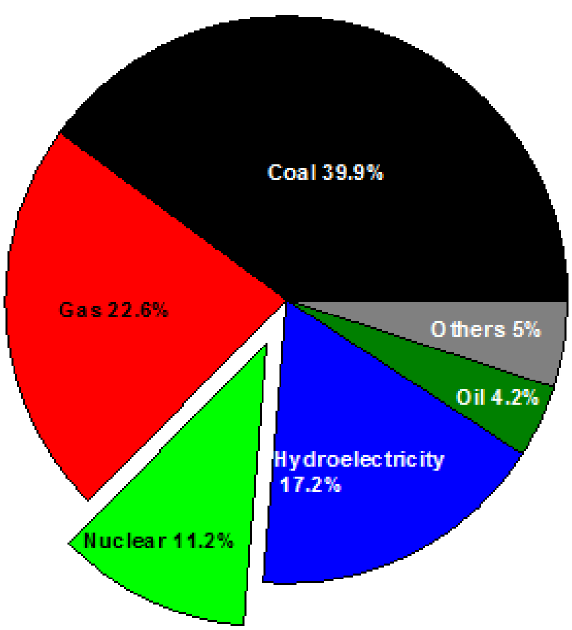

(a) World: Population 7,256 millions; EEC 19,710 TW h/year or 310 W/Capita; HDI 0.711 or HDI Rank 103

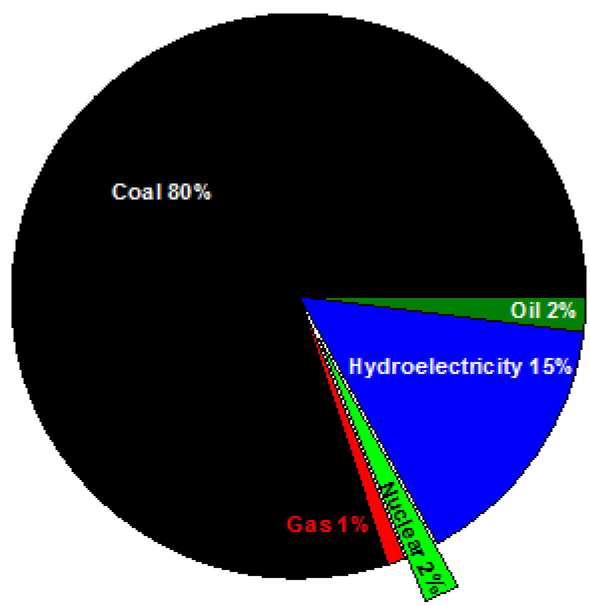

(b) China: Population 1,367 millions; EEC 5,523 TW h/year or 461 W/Capita; HDI 0.727 or HDI Rank 90

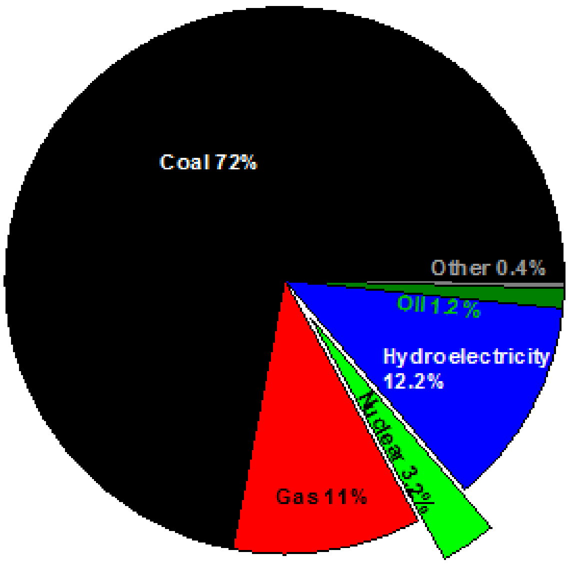

(c) India: Population 1,252 millions; EEC 865 TW h/year or 79 W/Capita; HDI 0.609 or HDI Rank 130

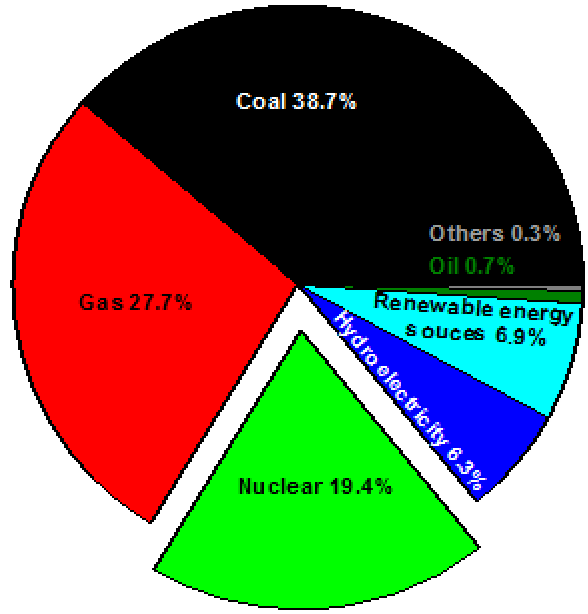

(d) USA: Population 321 millions; EEC 3,832 TW h/year or 1,360 W/Capita; HDI 0.915 or HDI Rank 8; Renewables (6.9%): Wind (4.4%); Biomass (1.7%); Geothermal (0.4%); and Solar (0.4%)

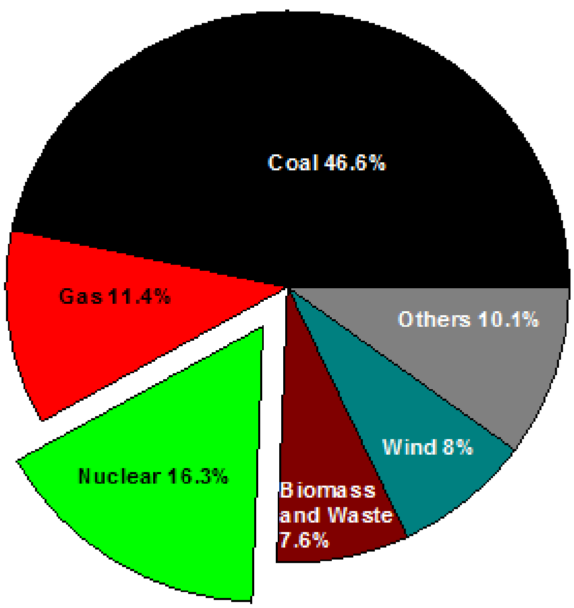

(e) Germany: Population 81 millions; EEC 540 TW h/year or 762 W/Capita; HDI 0.916 or HDI Rank 6

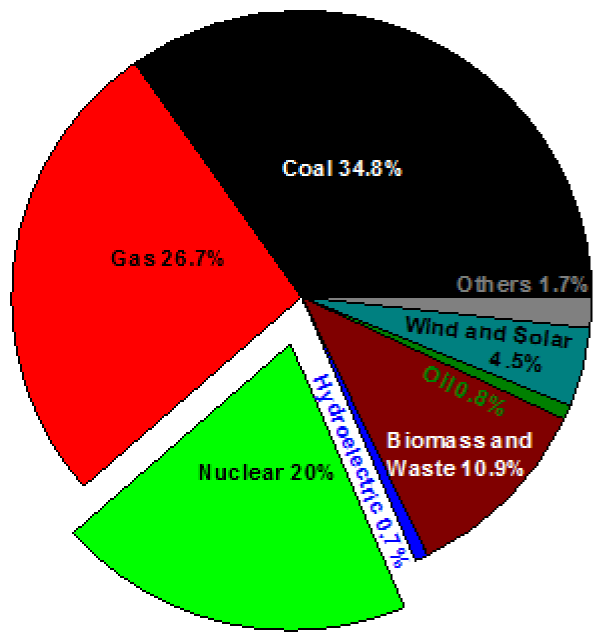

(f) UK: Population 64 millions; EEC 319 TW h/year or 568 W/Capita; HDI 0.907 or HDI Rank 14

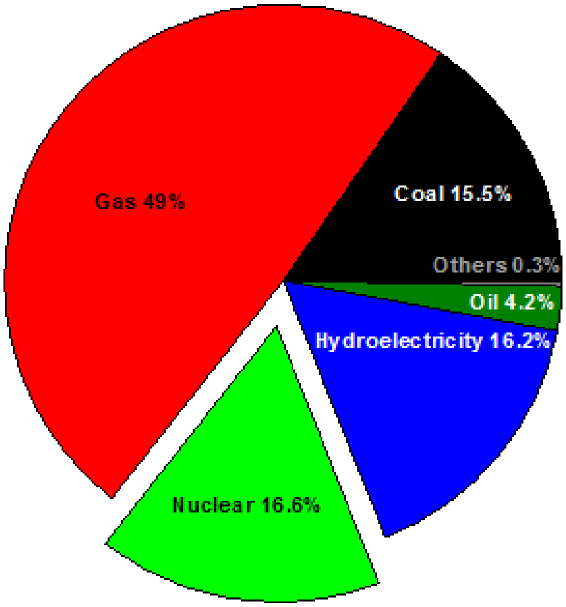

(g) Russia: Population 142 millions; EEC 1,037 TW h/year or 831 W/Capita; HDI 0.798 or HDI Rank 50

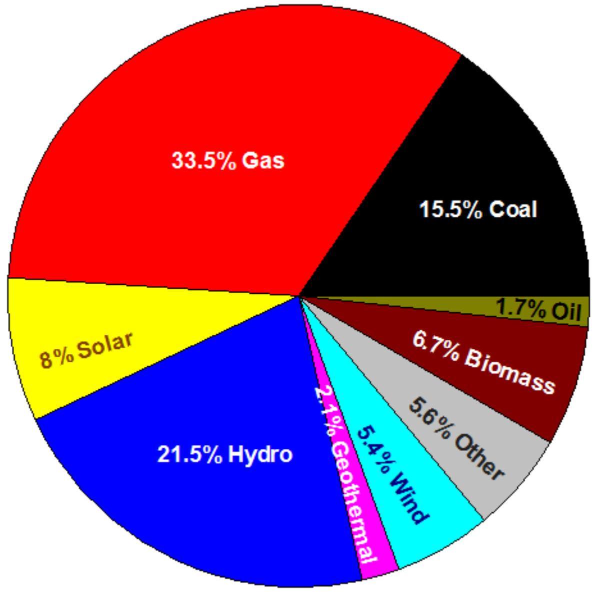

(h) Italy: Population 62 millions; EEC 303 TW h/year or 559 W/Capita; HDI 0.873 or HDI Rank 27

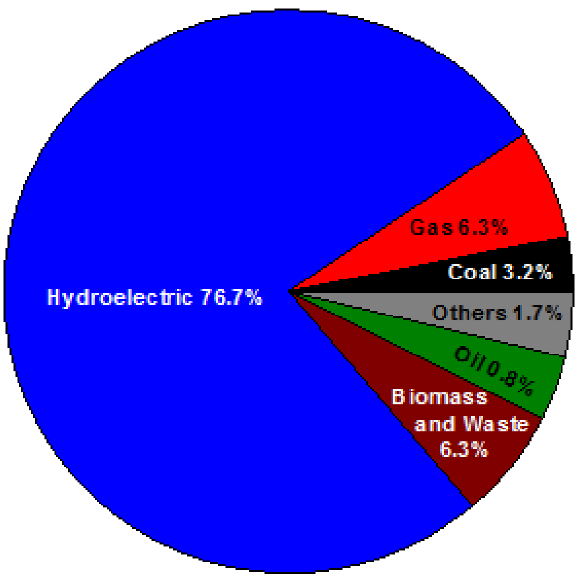

(i) Brazil: Population 204 millions; EEC 484 TW h/year or 270 W/Capita; HDI 0.755 or HDI Rank 75

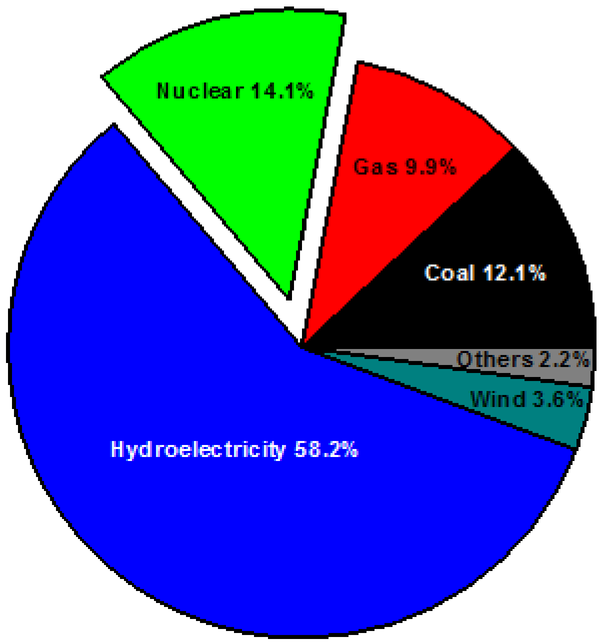

(j) Canada: Population 35 millions; EEC 525 TW h/year or 1,706 W/Capita; HDI 0.913 or HDI Rank 9

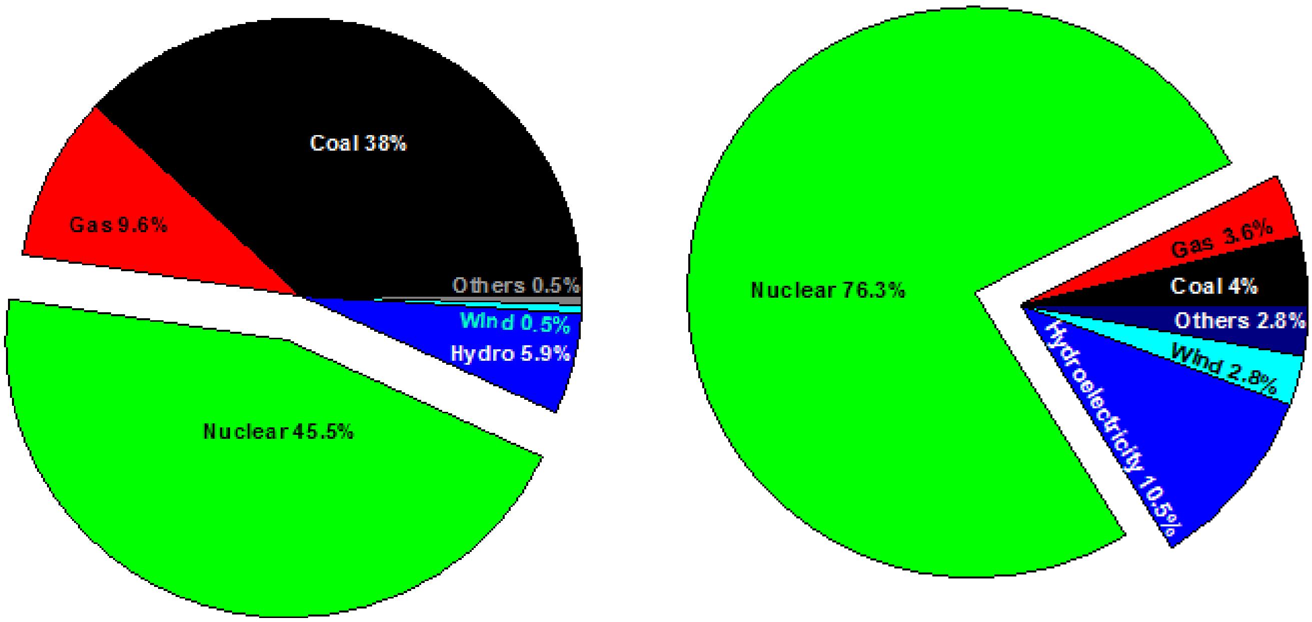

(k) Ukraine: Population 44 millions; EEC 160 TW h/year or 410 W/Capita; HDI 0.747 or HDI Rank 81

(l) France: Population 67 millions; EEC 451 TW h/year or 773 W/Capita; HDI 0.888 or HDI Rank 22

Figure 2 Electricity generation by source in the world and selected countries (data from 2010 – 2014 presented here just for reference purposes) [1]

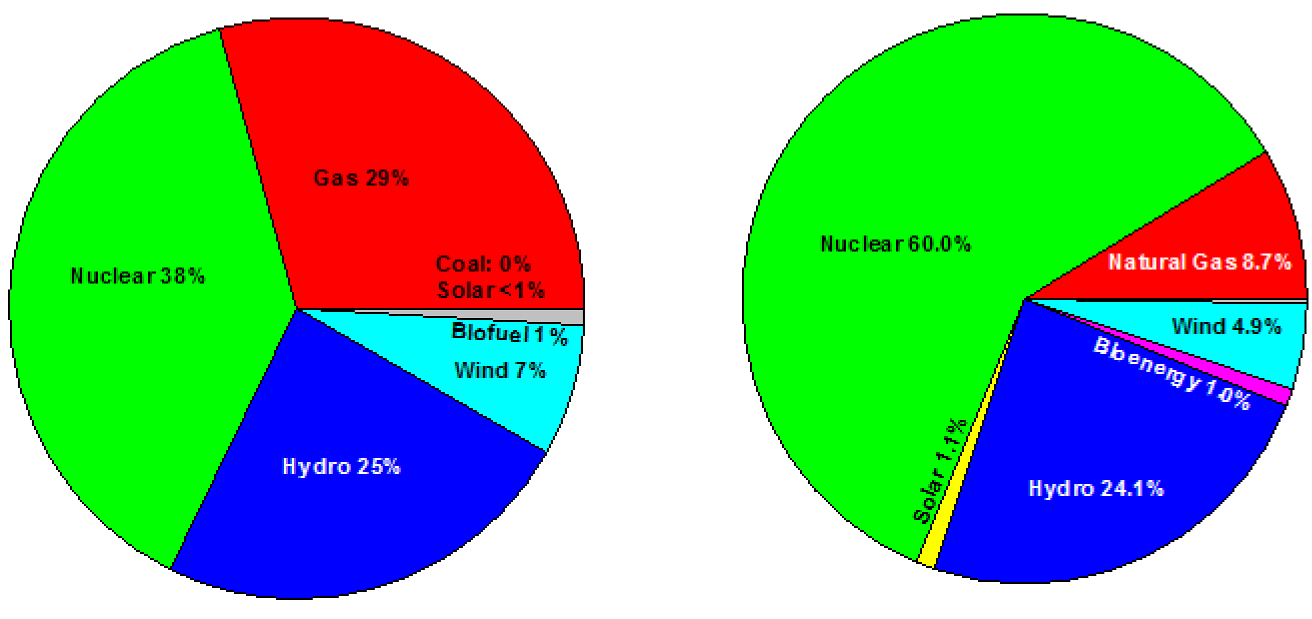

(a) **(b)**

Figure 3 Installed capacity (a) and electricity generation (b) by energy source in Ontario (Canada), 2014-2015 (based on data from Ontario Energy Board: http://www.ontarioenergyboard.ca/ and Ontario Energy Report http://www.ontarioenergyreport.ca/) [1]

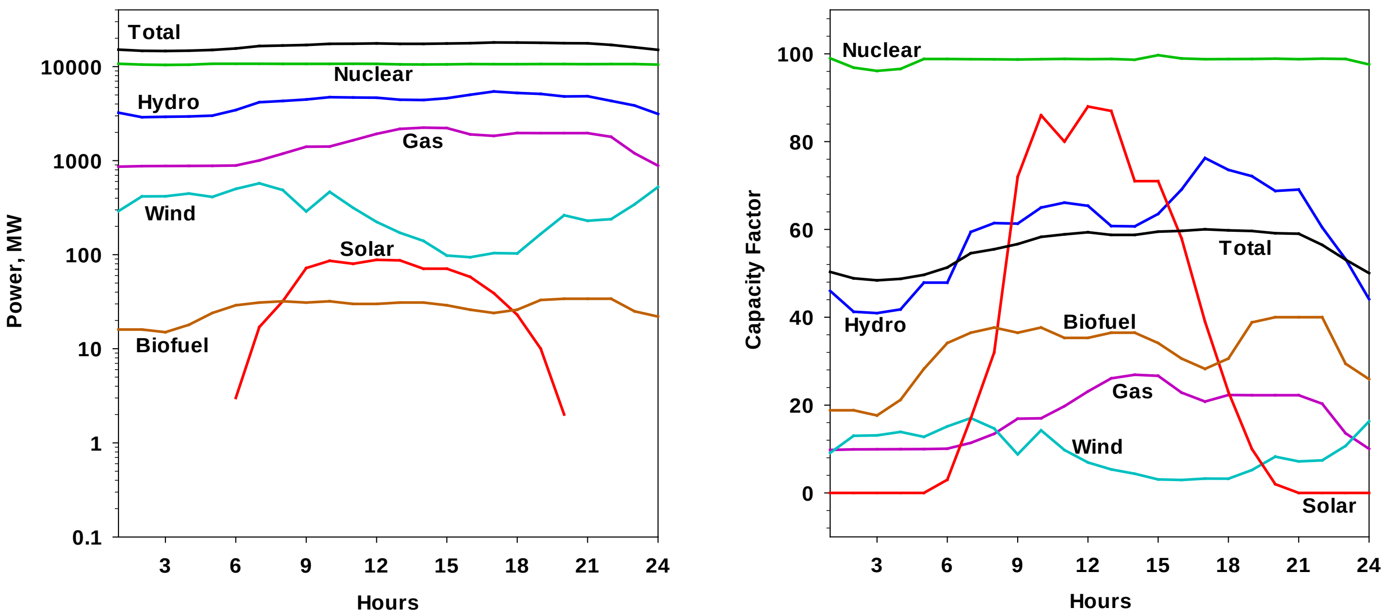

(a) (b)

Figure 4 Power generated (a) and capacity factors (b) of various energy sources in Ontario (Canada) on June 17, 2015 (based on data from http://ieso.ca/imoweb/marketdata/genEnergy.asp) (shown here just for reference purposes) [1]

Table 2 Eleven top power plants of the world by installed capacity[3] [1]

No	Plant	Country	Capacity MW_{el}	Average annual generation TWh	Capacity factor, %	Plant type
1	Three Gorges Dam	China	22,500	98.8	50	Hydro
2	Itaipu Dam	Brazil/Paraguay	14,000	98.6	72	Hydro
3	Xiluodu	China	13,860	57.1	47	Hydro
4	Guri Dam	Venezuela	10,200	-	-	Hydro
5	Tucurui Dam	Brazil	8,370	-	-	Hydro
6	Kashiwazaki-Kariwa	Japan	7,965	-	-	Nuclear
7	Grand Coulee Dam	USA	6,809	21.0	35	Hydro
8	Longtan Dam	China	6,426	18.7	33	Hydro
9	Sayano-Shushenskaya	Russia	6,400	24.0	43	Hydro
10	Bruce NPP	Canada	6,231	45.6	83	Nuclear
11	Krasnoyarsk Dam	Russia	6,000	23.0	44	Hydro

Currently, Bruce Nuclear Power Plant (NPP) is the largest fully-operating nuclear plant in the world.

Table 3 Largest operating power plants of the world (based on installed capacity) by energy source (Wikipedia, 2017) [1]

Rank	Plant	Country	Capacity, MW_{el}	Plant type
1	Three Gorges Dam Power Plant	China	22,500	Hydro
2	Bruce NPP	Canada	6,231	Nuclear
3	Taichung Power Plant	Taiwan	5,780	Coal
4	Shoaiba	S. Arabia	5,600	Fuel oil*
5	Surgut-2	Russia	5,597	Natural gas
6	Eesti Power Plant	Estonia	1,615	Oil shale

[3] Information provided in Table 2 is considered to be correct within some timeframe. New units can be added and/or some units can be out of service; for example, currently, i.e., May of 2017, the Kashiwazaki-Kariwa NPP is out of service after the earthquake and tsunami disaster and as the result – the severe accident at the Fukushima NPP in Japan in March of 2011.

Rank	Plant	Country	Capacity, MW_{el}	Plant type
7	Shatura Power Plant	Russia	1,500	Peat*
7	Gansu	China	5,160	Wind
8	Ivanpah Solar Power Facility	USA	392	Solar (thermal)
9	The Geysers	USA	1,808	Geothermal
10	Drax Power Plant	UK	660	Biofuel*
11	Sihwa Lake Tidal Power Plant	S. Korea	254	Tidal
12	Topaz	USA	550	Solar (PV**)
13	Vasavi Basin Bridge Diesel Power Plant	India	200	Diesel
14	Islay Limpet	UK	0.5	Marine (wave)***

* It should be noted that actually, some thermal power plants use multi-fuel options, for example, Surgut-2 (15% natural gas), Shatura (peat – 11.5%, natural gas – 78%, fuel oil – 6.8% and coal – 3.7%), Alholmens Kraft (primary fuel – biomass, secondary – peat and tertiary – coal) power plants. ** PV – PhotoVoltaic. ***Currently, not in operation anymore.

Table 4a Typical ranges of thermal efficiencies (gross) of modern thermal power plants [1]

No	Thermal Power Plant	Gross Eff., %
1	Combined-cycle power plant (combination of Brayton gas-turbine cycle (fuel - natural gas or LNG; combustion-products parameters at the gas-turbine inlet: T_{in}≈1650°C) and Rankine steam-turbine cycle (steam parameters at the turbine inlet: T_{in}≈620°C (T_{cr}=374°C)) (For details, see Fig. 7)	Up to 62
2	Supercritical-pressure coal-fired power plant (Rankine-cycle steam inlet turbine parameters: P_{in}≈23.5–38 MPa (P_{cr}=22.064 MPa), T_{in}≈540-625°C (T_{cr}=374°C) and T_{reheat}≈540-625°C) (For details, see Fig. 5)	Up to 55
3	Internal-combustion-engine generators (Diesel cycle and Otto cycle with natural gas as a fuel)	Up to 50
4	Subcritical-pressure coal-fired power plant (older plants) (Rankine-cycle steam: P_{in}≈17 MPa, T_{in}≈540°C (T_{cr}=374°C) and T_{reheat}≈540°C)	Up to 43
5	Concentrated-solar thermal power plants with heliostats, solar receiver (heat exchanger) on a tower and molten-salt heat-storage system: Molten-salt maximum temperature is about 565°C, Rankine steam-turbine power cycle used	Up to 20

Table 4b Typical ranges of thermal efficiencies (gross) of modern NPPs [1]

No	Nuclear Power Plant	Gross Eff., %
1	Carbon-dioxide-cooled reactor NPP (Generation-III) (reactor coolant: P=4 MPa & T=290-650°C; steam: P=16.7 MPa (T_{sat}=351°C and T_{cr}=374°C) & T_{in}=538°C; reheat: P=4.1 MPa & T_{in}=538°C)	Up to 42
2	Sodium-cooled fast reactor NPP (Generation-IV) (steam: P=14 MPa (T_{sat}=337°C) & T_{in}=505°C and reheat: P=2.45 MPa & T_{in}=505°C) (For details, see Fig. 9)	Up to 40
3	Pressurized Water Reactor NPP* (Generation-III+, to be implemented within next 1-10 years) (reactor coolant: P=15.5 MPa & T_{out}=327°C; steam: P=7.8 MPa & T_{in}=T_{sat}=293°C and reheat)	Up to 38
4	Pressurized Water Reactor NPP* (Generation-III, current fleet) (reactor coolant: P=15.5 MPa & T_{out}=329°C; steam: P=6.9 MPa & T_{in}=T_{sat}=285°C and reheat) (For details, see Fig. 8)	Up to 36
5	Boiling Water Reactor NPP* (Generation-III, current fleet) (direct cycle) (P_{in}=7.2 MPa & T_{in}=T_{sat}=288°C and reheat)	Up to 34
6	RBMK NPP*(boiling, pressure-channel) (Generation-III, current fleet) (direct cycle) (P_{in}=6.46 MPa & T_{in}=T_{sat}=280°C; reheat: P=0.29 MPa & T_{reheat}=263°C)	Up to 32
7	Pressurized Heavy Water Reactor NPP* (Generation-III, current fleet) (reactor coolant: P=11 MPa & T=260-310°C; steam: P=4.6 MPa & T_{in}=T_{sat}=259°C and reheat)	Up to 32

Note to table: 1) All NPPs with water-cooled reactors use only Rankine cycle with saturated steam at the inlet of a turbine and steam reheat, which uses primary saturated steam as the heating medium.

Table 5 Average (typical) capacity factors of various power plants (listed here just for reference purposes) (partially based on (US Energy Information Administration, 2013) [1]

No	Power Plant type	Location	Year	Capacity factor, %
1	Nuclear	USA	2010	91
		UK	2011	66
2	Combined-cycle	USA	2009	42
		UK	2011	48
3	Coal-fired	USA	2009	64
		UK	2011	42
4	Hydroelectric[4]	USA and UK	2011	40
		World (average)	-	44
		World (range)	-	10-99
5	Wind	UK	2011	30
		World	2008	20-40
6	Wave	Portugal	-	20
7	Concentrated-solar thermal	USA California Spain	- -	21 75
8	Photovoltaic (PV) solar	USA Arizona	2008	19
		USA Massachusetts	-	12-15
		UK	2011	5-8
9	Concentrated-solar PV	Spain	-	12

These examples show clearly that any grid that includes NPPs and/or renewable-energy sources must also include "fast-response" power plants such as gas- and coal-fired and/or large hydro-power plants. This is due not only to diurnal and seasonal peaking of demand, but also the diurnal and seasonal variability of supply. Thus, for any given market, the generating mix and the demand cycles must be matched 24/7/365, independent of which sources are used, and this requires flexible control and an appropriate mix of base-load and peaking plants.

Also, it should be noted here that having a large percent of variable power sources mainly such as wind and solar, and other, i.e., which generating capacity depends on Mother Nature, an electrical grid can collapse due to significant and unpredicted power instabilities! In addition, the following detrimental factors are usually not considered during estimation of variable power-sources costs: 1) costs of fast-response power plants with service crews on site 24/7 as a back-up power and 2) faster amortization / wear of equipment of fast-response plants.

2. THERMAL POWER PLANTS

In general, all thermal power plants [1, 3] are based on one the following thermodynamic cycles see also, Table 4a):

1) Rankine steam-turbine cycle (the mostly widely-used in various power plants; usually, for solid, gaseous and liquid fuels, but other energy sources can be also used, for example, geothermal, solar, etc.) (see Figs. 5 and 6);

2) Brayton gas-turbine cycle (the second one after the Rankine cycle in terms of application in power industry; only for clean gaseous fuels);

3) Combined Cycle, i.e., combination of Brayton and Rankine cycles in one plant (only for gaseous fuels) (see Fig. 7);

4) Diesel internal-combustion-engine cycle (for Diesel fuel used in Diesel generators); and

5) Otto internal-combustion-engine cycle (usually, for natural or liquefied gas, but also, gasoline can be used for power generation; however, it is more expensive fuel compared to gaseous fuels) and also, used in internal-combustion-engine generators.

The major driving force for all advances in thermal power plants is directed towards increasing thermal efficiency in order to reduce operating fuel costs and minimize specific emissions. Typical ranges of thermal efficiencies of modern thermal power plants are listed in Table 4a for reference purposes and can reach up to 62% in the combined-cycle mode.

It should be noted that from the thermodynamic point of view it is known in which direction we have to move, i.e., towards higher temperatures and pressures. However, we are limited by strength and costs of materials, which can withstand these harsh conditions!

In general, for supercritical-pressure coal-fired power plants as the most efficient plants with Rankine cycle current ranges of pressures are 23.5 – 38 MPa and inlet temperatures to high-pressure turbine up to 625°C and secondary steam (steam reheat) is also up to 625°C. For gas turbines – inlet temperatures to turbine are up to 1650°C.

[4] Capacity factors depend significantly on a design, size and location (water availability) of a hydroelectric power plant. Small plants built on large rivers will always have enough water to operate at a full capacity.

Unfortunately, information on supercritical-pressure thermal power plants the latest advanced operating conditions of combined-cycle and other power plants are completely missed in the vast majority of modern textbooks on thermodynamics. Moreover, heat transfer at supercritical pressures is missed in the vast majority of heat-transfer textbooks and handbooks!

Despite the all advances in thermal power-plants design and operation worldwide, they are still considered as not of minimum environmental impact due to significant carbon-dioxide emissions[5] and air pollution as a result of the combustion process. In addition, coal-fired power-plants produce also virtual mountains of slag and ash, and other gas emissions may contribute to acid rains.

New developments in solar thermal power plants are using molten salt in the primary circuit or organic fluid [1]. As such Gemasolar - a 19.9-MW_{el} concentrated solar thermal power plant with a 140-m high tower and molten-salt heat-storage system was built in Spain. This plant consists of 2,650 heliostats (each 120 m^2 and total reflective area 304,750 m^2), covers 1.95 km^2 (195 ha) and produces 110 GW h annually, which equals to 30,000 t/year carbon-dioxide emission savings. This energy is enough to supply 25,000 average Spanish houses. The storage system allows the power plant to produce electricity for 15 h without sunlight (at night or on cloudy days). Due to this its capacity factor is 75%! Solar-receiver thermal power is 120 MW_{th}, and plant thermal efficiency is about 19%. Molten salt is heated in the solar receiver from 260 to 565°C by concentrated sun light reflected from all heliostats, which follow the sun, and transfers heat in a steam generator to water as the working fluid in a subcritical-pressure Rankine steam-power cycle.

3. MODERN NUCLEAR POWER PLANTS

Although nuclear power is often considered to be a non-renewable-energy source as the fossil fuels, like coal and gas, nuclear resources can be used for significantly longer or even indefinite time than some fossil fuels, especially, if recycling of unused uranium fuel, and thoria-fuel resources and fast reactors will be used. Major advantages of nuclear power [1, 4, 5] are:

1) High capacity factors are achievable, often in excess of 90% with long operating cycles, making the units suitable for semi-continuous base-load operation, alongside intermittent windmills backed by gas peaking plants.

2) Essentially negligible operating emissions of carbon dioxide into atmosphere compared to alternate thermal plants;

2) Relatively small amount of fuel required (for example, a 500-MW_{el} coal-fired supercritical-pressure power plant requires 1.8 million ton of coal annually, but a fuel load into a 1300-MW_{el} Pressurized Water Reactor (PWR) is 115 t (3.2% enrichment) or into a 1330-MW_{el} Boiling Water Reactor (BWR) – 170 t (1.9% enrichment)). Therefore, this source of energy is considered as the most viable one for electrical generation for the next 50 – 100 years. Unfortunately, any information on NPPs is completely missed in the vast majority of modern thermodynamic textbooks.

It should be noted that the vast majority of current NPPs are equipped with water-cooled reactors (96% of 444 nuclear-power reactors), which use only subcritical-pressure Rankine steam-power cycle with saturated primary steam (maximum pressures about 7 MPa and saturation temperature about 286°C) and steam reheat, which uses primary saturated steam as the heating medium (see Fig. 8). Due to this the maximum thermal efficiencies achieved are about 36% gross.

There are only 14 Advanced Gas-cooled Reactors (AGRs) left in UK, which connected through steam generators with subcritical-pressure Rankine steam-power cycle (for details on AGRs and steam parameters, see Table 4b). NPPs with AGRs have reached the highest thermal efficiencies in the nuclear-power industry of about 42%. Unfortunately, all these reactors will be shut down within next 10–15 years and never will be built again! Second highest thermal efficiencies in nuclear-power industry (about 40%) are related to NPPs equipped with Sodium-cooled Fast Reactors (SFRs) (see Fig. 9). Currently, only two SFRs are in operation in Russia.

In spite of all current advances in nuclear power, NPPs have the following deficiencies: 1) Generate radioactive wastes; 2) Have relatively low thermal efficiencies, especially, water-cooled NPPs (up to 1.6 times lower than that for modern advanced thermal power plants (see Tables 4b and 4a)); 3) Risk of radiation release during severe accidents; and 4) Production of nuclear fuel is not an environment-friendly process. Therefore, all these deficiencies should be addressed in the next generation nuclear-power reactors and NPPs.

4. NEXT GENERATION NUCLEAR POWER PLANTS

The demand for clean, non-fossil-based electricity is growing; therefore, the world needs to develop new nuclear reactors / NPPs with higher thermal efficiencies in order to increase electricity generation and decrease detrimental effects on the environment.

Currently, a group of countries, including Canada, EU, Japan, Russia, USA and others have initiated an international collaboration to develop the next generation nuclear reactors (Generation IV reactors). The ultimate goal of developing such reactors is an increase in thermal efficiencies of NPPs from 30 - 36% to 45 - 50% and even higher. This increase in thermal efficiency would result in a higher generation of electricity compared to current Light-Water-Reactor (LWR) technologies per 1 kg of uranium.

The Generation IV International Forum (GIF) Program has narrowed design options of nuclear reactors to six concepts [1, 6]. These concepts are: 1) Gas-cooled Fast Reactor (GFR) or just High Temperature Reactor (HTR), 2) Very High Temperature Reactor (VHTR), 3) Sodium-cooled Fast Reactor (SFR), 4) Lead-cooled Fast Reactor (LFR), 5) Molten Salt Reactor (MSR), and 6) SuperCritical Water-cooled Reactor (SCWR).

[5] For example, the largest in the world 5,780-MW_{el} Taichung coal-fired power plant (Taiwan) is the world's largest emitter of carbon dioxide with over 40 million tons per year.

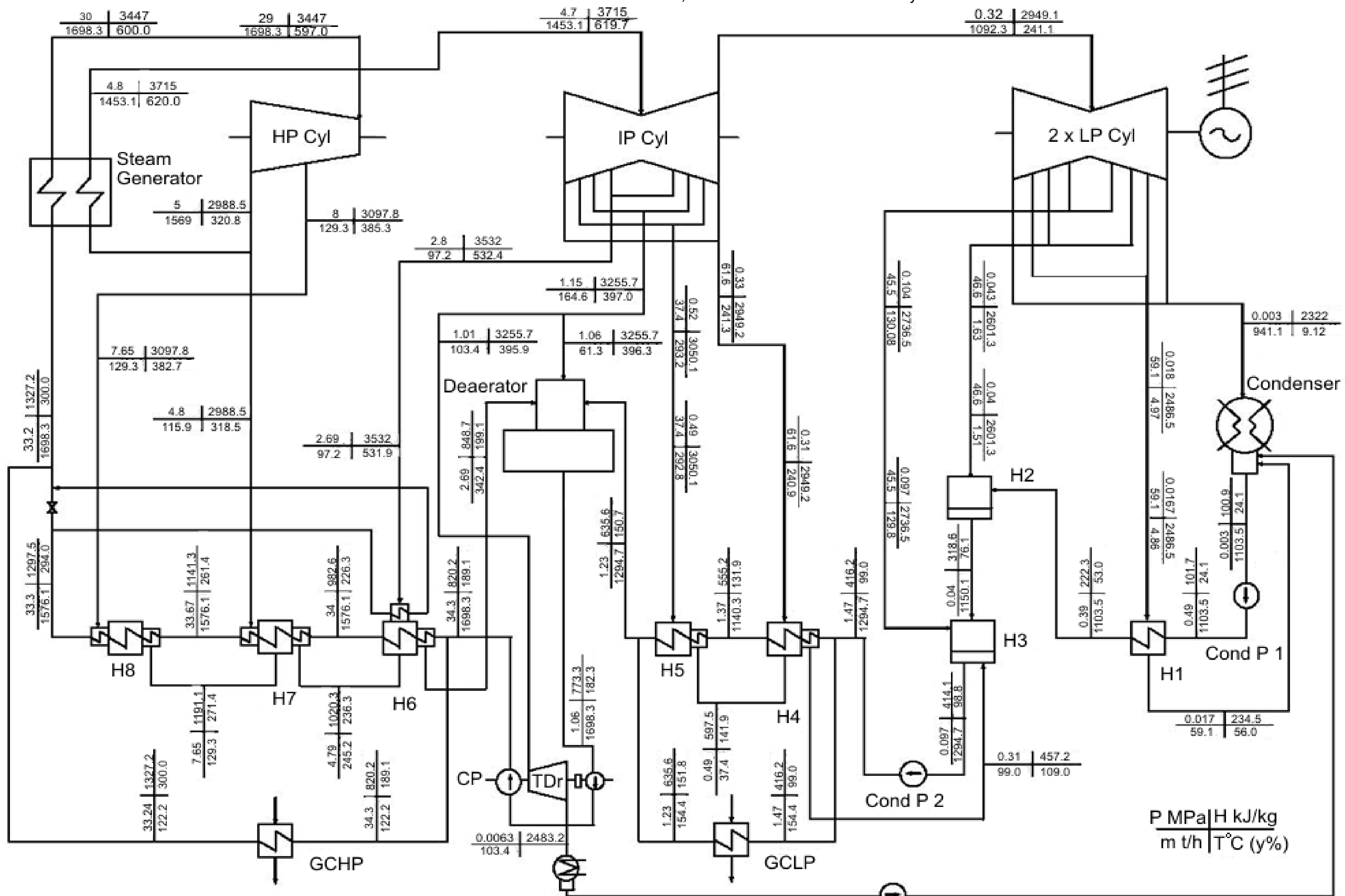

Figure 5 Single-reheat-regenerative cycle 600-MW$_{el}$ Tom'-Usinsk thermal power plant (Russia) layout (Kruglikov et al., TsKTI, Russia, 2009) [1]: Cyl – Cylinder; H – Heat exchanger (feedwater heater); CP – Circulation Pump; TDr – Turbine Drive; Cond P – Condensate Pump; GCHP – Gas Cooler of High Pressure; and GCLP – Gas Cooler of Low Pressure. (For *T-s* diagram, see Fig. 6)

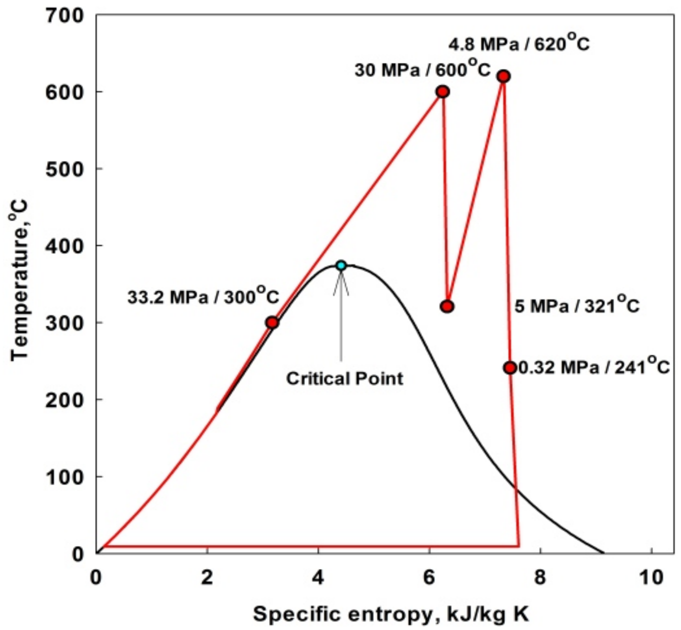

Figure 6 Simplified *T-s* diagram for Tom'-Usinsk thermal-power-plant supercritical-pressure Rankine steam-turbine cycle [1]

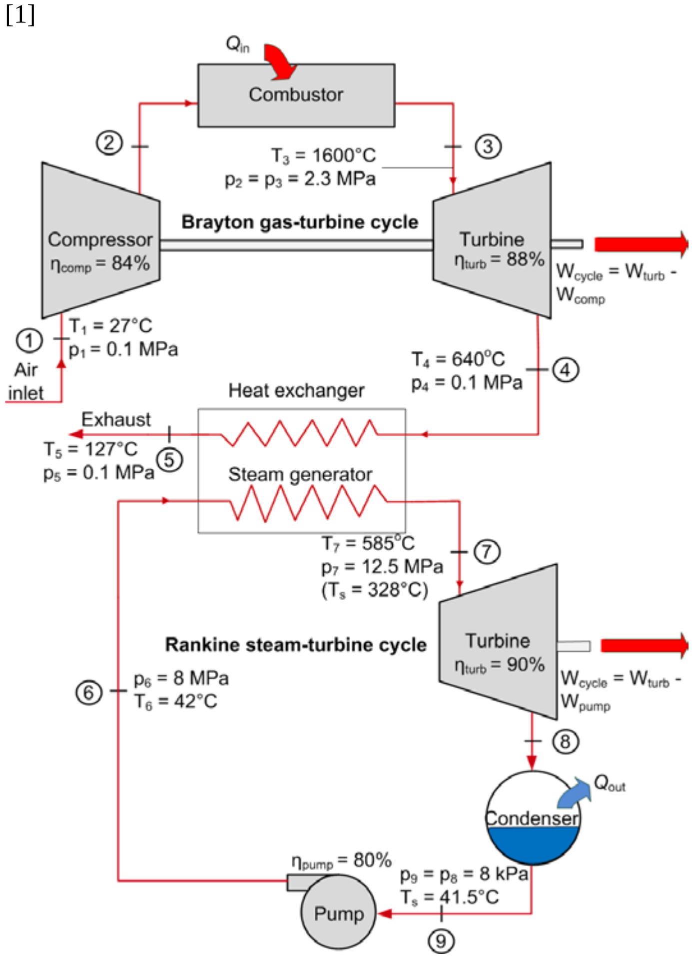

(a)

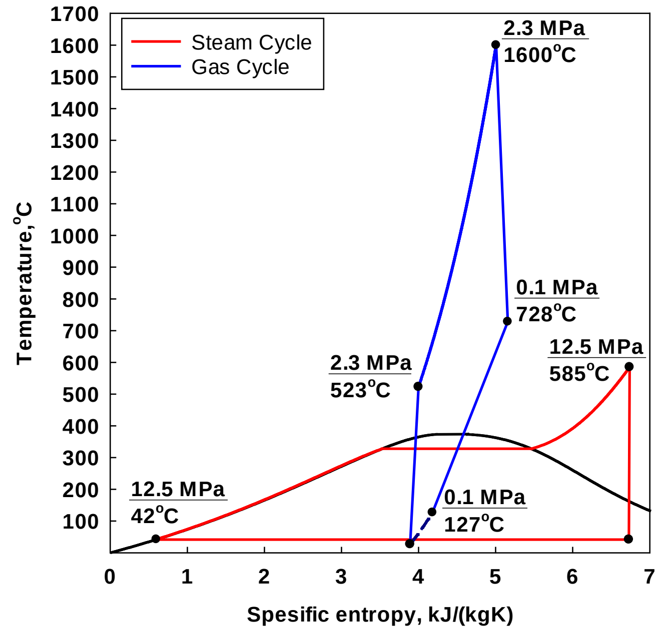

(b)

Figure 7 Modern combined-cycle power plant schematic (a) and *T-s* diagram (b) (partially based on data from Mitsubishi Heavy Industries (MHI) and Siemens) [1]

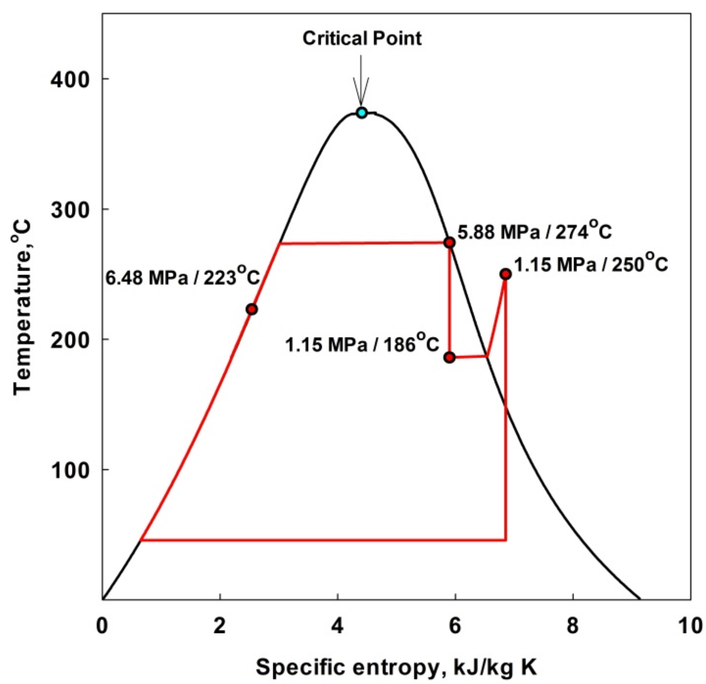

Figure 8 Temperature – Specific Entropy diagram for Pressurized Water Reactor (PWR) NPP typical turbine cycle [1]

Thermal efficiencies of NPPs equipped with Generation-IV nuclear-power reactors are listed in Table 6 and selected layout and *T-s* diagrams – in Figs. 10–12.

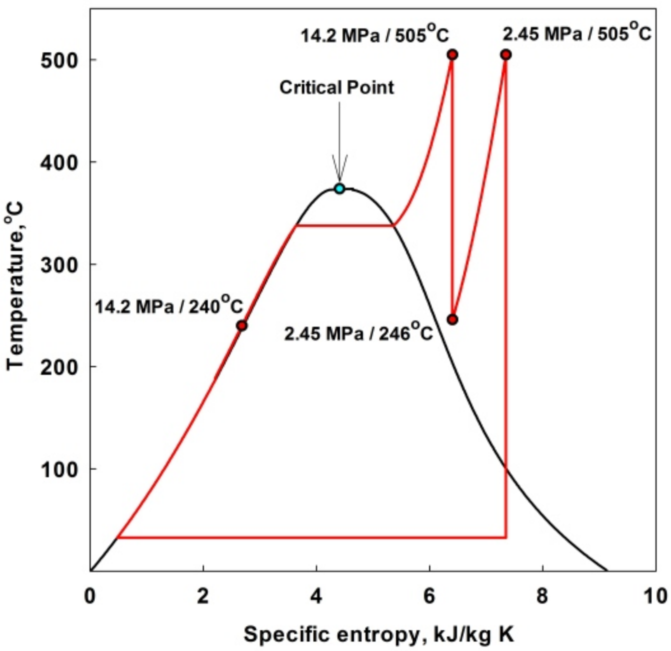

Figure 9 *T*–*s* diagram for 600-MW_{el} Sodium-cooled Fast Reactor (SFR) NPP typical turbine cycle [1]

Table 6 Estimated ranges of thermal efficiencies (gross) of Generation-IV NPP concepts [1, 6]

No	Nuclear Power Plant	Thermal Eff., %
1	Very High Temperature Reactor (VHTR) NPP (reactor coolant – helium: P=7 MPa and T_{in}/T_{out}=640/1000°C; primary power cycle – direct Brayton gas-turbine cycle; possible back-up – indirect Brayton cycle(s), combined cycle or Rankine steam cycle) (For details, see Figs. 10–12)	≥55
2	Gas-cooled Fast Reactor (GFR) NPP (reactor coolant – helium: P=9 MPa and T_{in}/T_{out}=490/850°C; primary power cycle – direct Brayton gas-turbine cycle; possible back-up – indirect Brayton cycle(s), combined cycle or Rankine steam cycle).	≥50
3	SuperCritical Water-cooled Reactor (SCWR) NPP (one of Canadian concepts; reactor coolant – light water: P=25 MPa and T_{in}/T_{out}=350/625°C (T_{cr}=374°C); direct cycle; high-temperature steam superheat: T_{out}=625°C; possible back-up – indirect SuperCritical Pressure (SCP) Rankine "steam" cycle with high-temperature steam superheat)	45–50
4	Molten Salt Reactor (MSR) NPP (reactor coolant – sodium-fluoride salt with dissolved uranium fuel: T_{out}=700–800°C; primary power cycle – indirect SCP carbon-dioxide Brayton gas-turbine cycle; possible back-up – SCP Brayton gas-turbine cycle with other working fluids or combined cycle)	~50%
5	Lead-cooled Fast Reactor (LFR) NPP (Russian design Brest-300: reactor coolant – liquid lead: P≈0.1 MPa and T_{in}/T_{out}=420/540°C; primary power cycle – indirect subcritical- (~18 MPa) or SCP Rankine "steam" cycle: P_{in}≈24.5 MPa (P_{cr}=22.064 MPa) and T_{in}/T_{out}=340/520°C (T_{cr}=374°C); high-temperature steam superheat; possible back-up in some other countries – indirect SCP carbon-dioxide Brayton gas-turbine cycle)	~43
6	Sodium-cooled Fast Reactor (SFR) NPP (Russian design BN-600: reactor coolant – liquid sodium (primary circuit): P≈0.1 MPa and T_{in}/T_{out}=380/550°C; liquid sodium (secondary circuit): T_{in}/T_{out}=320/520°C; primary power cycle – indirect Rankine steam cycle: P_{in}≈14.2 MPa (T_{sat}≈337°C) and $T_{in\ max}$=505°C (T_{cr}=374°C); steam superheat: P≈2.45 MPa and T_{in}/T_{out}=246/505°C; possible back-up in some other countries – indirect SCP carbon-dioxide Brayton gas-turbine cycle) (For details, see Fig. 9)	Up to 40–42

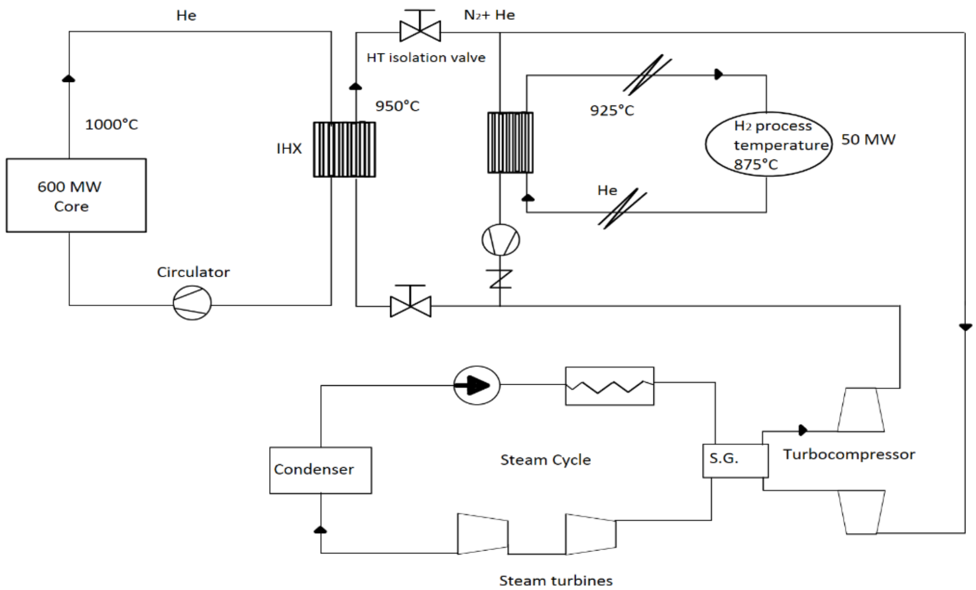

Figure 10 Simplified schematic of VHTR NPP (reactor coolant – helium at 5 MPa) with indirect combined cycle (Primary – Brayton gas-turbine cycle (working fluid – mixture of nitrogen and helium at 5 MPa) and Secondary – Rankine steam-turbine cycle) and hydrogen co-generation (based on schematic from Gauthier et al. (2004)) [7]: HT – Heat Transfer; S.G. – Steam Gemerator.

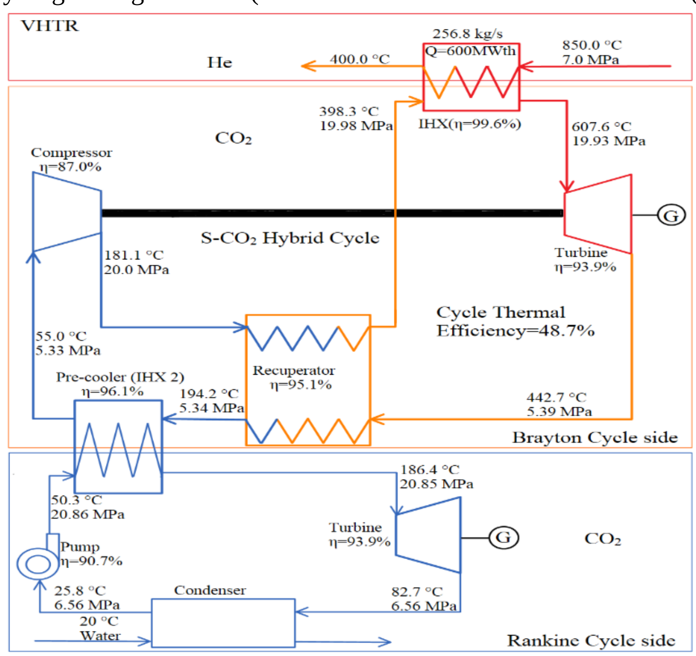

Figure 11 Simplified schematic of VHTR NPP (reactor coolant – helium at 7 MPa) with indirect combined cycle (Primary – SuperCritical Pressure (SCP) Brayton gas-turbine cycle (working fluid – carbon dioxide at ~20 MPa) and Secondary – SCP Rankine cycle (working fluid – carbon dioxide at ~21 MPa)) (based on schematic from Bae et al. (2014)) [7]. *T-s* diagram of this cycle is shown in Fig. 12: G – Generator; IHX – Intermediate Heat eXchanger; S-CO_2 – Supercritical CO_2

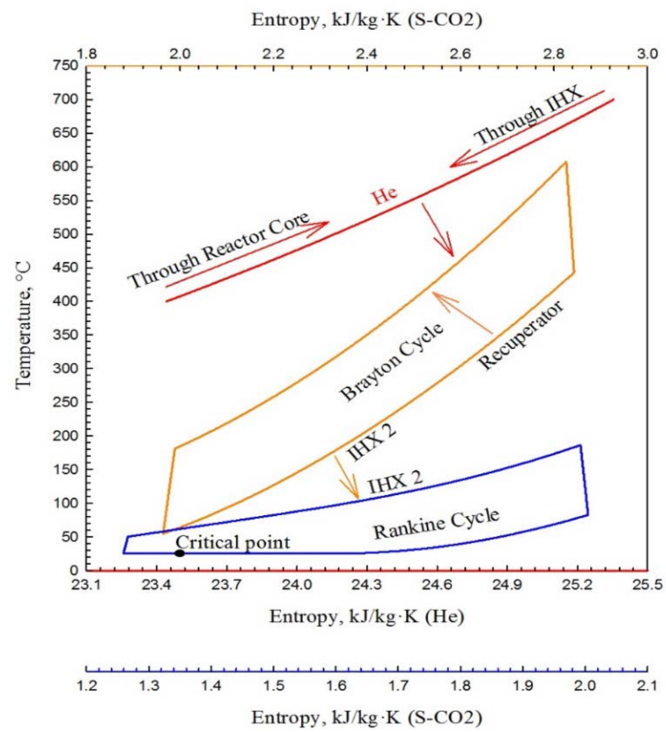

Figure 12 *T-s* diagram of VHTR NPP indirect combined power cycle with SCP carbon dioxide in Brayton and Rankine cycles (based on diagram from Bae et al. (2014)) [7]. For details, see schematic in Fig. 11

5. SPECIFICS OF THERMOPHYSICAL PROPERTIES, HEAT TRANSFER AND PRESSURE DROP AT SUPERCRITICAL PRESSURES

Based on the abovementioned it is clear that to reach higher thermal efficiencies power plants have to operate at high temperatures and pressures including supercritical ones [1, 8]. At critical and supercritical pressures a fluid is considered as a single-phase substance in spite of the fact that all thermophysical properties undergo significant changes within the critical and pseudocritical regions (see Figs. 13 and 14) [7, 9, 10]. Near the critical point, these changes are dramatic. In the vicinity of pseudocritical points, with an increase in pressure, these changes become less pronounced.

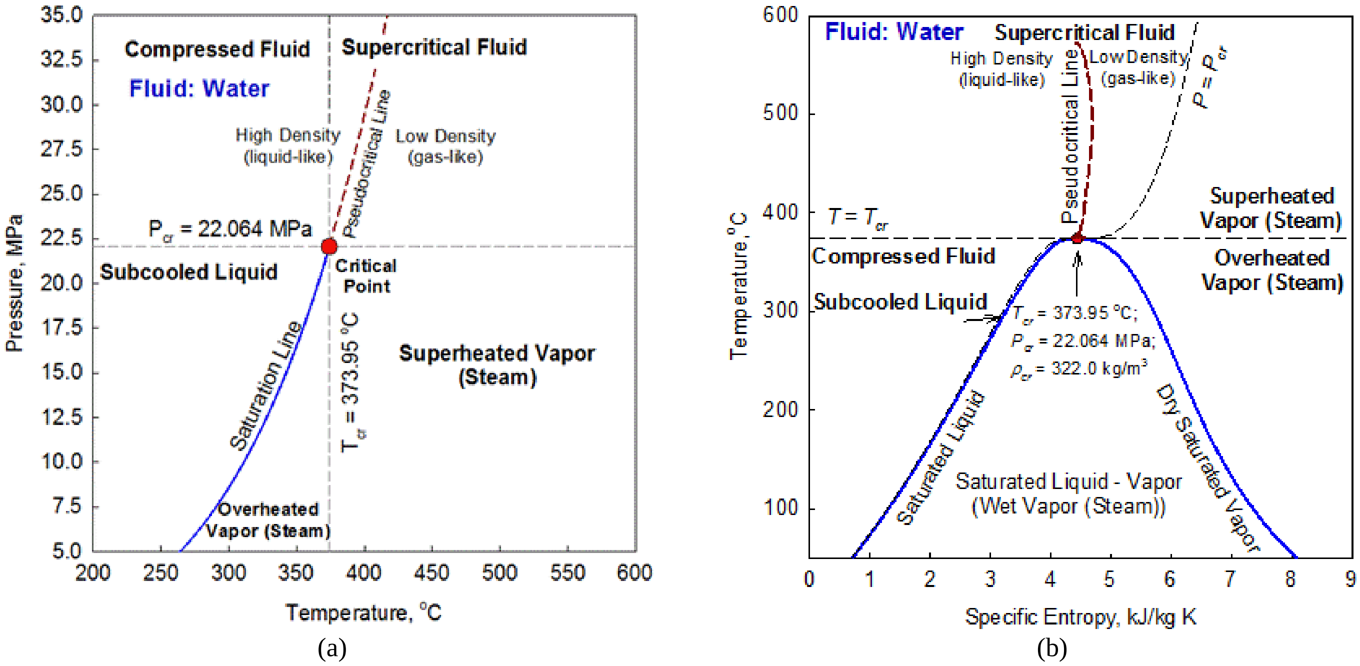

Figure 13 Thermodynamics diagrams for water: (a) Pressure–Temperature and (b) Temperature–Specific Entropy (based on [7])

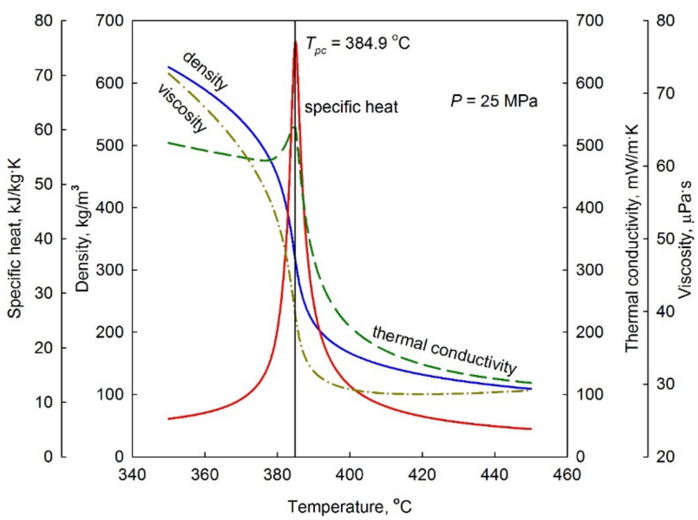

Figure 14 Profiles of Thermal Conductivity, Specific Heat, Density, and Dynamic Viscosity vs. Temperature (based on [7]: Supercritical water at pressure of 25 MPa. Pseudocritical region is about ±25°C around pseudocritical point

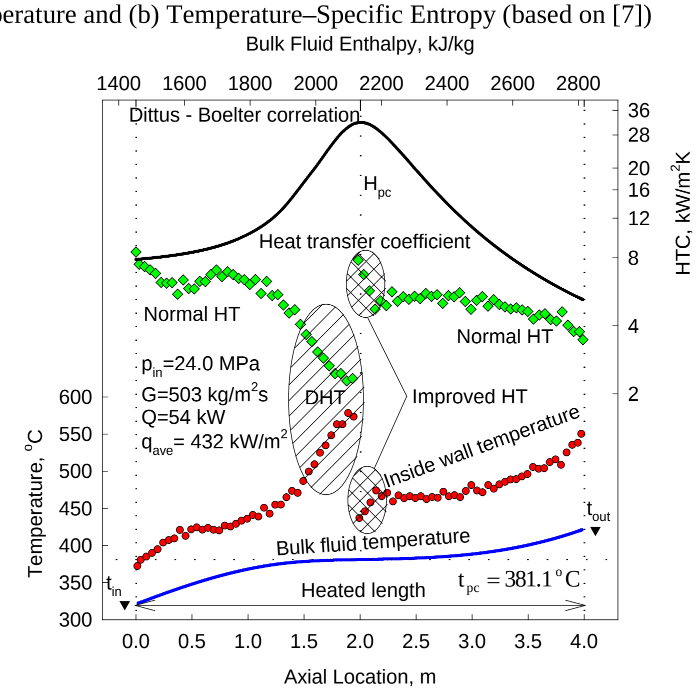

Figure 15 Temperature and Heat-Transfer-Coefficient (HTC) profiles along heated length of vertical bare circular tube cooled with supercritical water (data by Kirillov et al. (2003)) [11]: *ID* = 10 mm and L_h = 4 m

Specifics of thermophysical properties affect the heat transfer at supercritical pressures. In general, three major heat-transfer regimes can be identified at critical and supercritical pressures [1, 10, 11, 12] (for details, see Fig. 15): 1) Normal Heat Transfer (NHT); 2) Improved Heat Transfer (IHT); and 3) Deteriorated Heat Transfer (DHT). Also, two special phenomena may appear along a heated surface: 1) pseudo-boiling; and 2) pseudo-film boiling.

Due to these specifics in properties and heat transfer the well-known at subcritical pressures the Dittus-Boelter correlation significantly can overestimate heat transfer coefficients within the IHT regime. Therefore, a number of empirical heat-transfer correlations has been proposed for supercritical pressures.

In general, many of these correlations are based on the conventional Dittus-Boelter-type correlation in which the regular specific heat in Prandtl number is replaced with the cross-sectional averaged specific heat ($c_{p\ ave}$) or ($\bar{c}_p$) within the range of ($T_w - T_b$); $\left(\frac{H_w - H_b}{T_w - T_b}\right)$, J/kg K. In this case, the cross-sectional averaged Prandtl number ($\mathbf{Pr}_{ave}$) or ($\overline{\mathbf{Pr}}$) is $\left(\frac{\mu\,\bar{c}_p}{\rho}\right)$. Also, additional terms, such as: $\left(\frac{k_b}{k_w}\right)^k$; $\left(\frac{\mu_b}{\mu_w}\right)^m$; $\left(\frac{\rho_b}{\rho_w}\right)^n$; etc., can be added into correlations to account for significant variations in thermophysical properties within a cross section due to a non-uniform temperature profile, i.e., due to heat flux.

Therefore, the following correlations have been developed.

1) Correlation for SuperCritical Water (SCW) flowing inside vertical bare tubes, which is based on the bulk-fluid-temperature approach and cross-section-averaged specific heat, is as the following [1, 11, 12]]:

$$\mathbf{Nu_b} = 0.0061\ \mathbf{Re_b^{0.904}}\ \overline{\mathbf{Pr}}_\mathbf{b}^{0.684}\left(\frac{\rho_w}{\rho_b}\right)^{0.564}. \qquad (1)$$

Correlation (Eq. (1)) is the most accurate heat-transfer correlation for SCW forced convection compared to other heat-transfer correlations: Uncertainty ±25% for Heat Transfer Coefficient (HTC) values and ±15% for wall temperatures. This correlation was verified within the following operating conditions: Water, upward flow, vertical bare tubes with inside diameter 3 – 38 mm, pressure 22.8 – 29.4 MPa, mass flux 200 – 3000 kg/m^{2}s, and heat flux 70 – 1250 kW/m^2. Also, Eq. (1) showed very good predictions for subcritical liquid (second by an RMS error after the Gnielinski (1976) correlation) and the most accurate for superheated steam compared to other correlations.

However, it should be noted that Eq. (1), as well as many other supercritical fluids heat-transfer correlations, can predict only HTC values at the NHT and IHT regimes. Unfortunately, there are no reliable correlations to predict HTCs at the DHT regime.

2) Nevertheless, the following empirical correlation for SCW was proposed for calculating the minimum heat flux at which the DHT regime appears in forced convection in bare vertical tubes with upward flow [8, 11]:

$$q_{dht} = -58.97 + 0.745 \cdot G\text{, kW/m}^2. \qquad (2)$$

Correlation (Eq. (2)) is valid within the following range of experimental parameters: Water, upward flow, vertical bare tube with inside diameter 10 mm, pressure 24 MPa, mass flux 200 – 1500 kg/m^{2}s, and bulk-fluid inlet temperature 320 – 350°C: Uncertainty ±15% for the DHT heat flux.

In general, the total pressure drop for forced convection can be calculated according to the following expression [1, 8, 10, 13]:

$$\Delta p = \sum \Delta p_{fr} + \sum \Delta p_\ell + \sum \Delta p_{ac} + \sum \Delta p_g\ , \qquad (3)$$

where Δp is the total pressure drop, in Pa.

The pressure drop due to frictional resistance, Δp_{fr} (Pa), is defined as:

$$\Delta p_{fr} = \left(\xi_{fr}\ \frac{L}{D}\frac{\rho u^2}{2}\right) = \left(\xi_{fr}\ \frac{L}{D}\frac{G^2}{2\rho}\right), \qquad (4)$$

where ξ_{fr} is the frictional coefficient, which can be obtained from appropriate correlations for different flow geometries. For smooth circular tubes, ξ_{fr} is:

$$\xi_{fr} = \left(\frac{1}{(1.82 \log_{10} \mathbf{Re_b} - 1.64)^2}\right). \qquad (5)$$

Equation (5) is valid within a range of $\mathbf{Re} = 4 \cdot 10^3 - 10^{12}$.

The pressure drop due to local flow obstruction, Δp_ℓ is (Pa), is defined as:

$$\Delta p_\ell = \left(\xi_\ell\ \frac{\rho u^2}{2}\right) = \left(\xi_\ell\ \frac{G^2}{2\rho}\right), \qquad (6)$$

where ξ_ℓ is the local resistance coefficient, which can be obtained from appropriate correlations for different flow obstructions.

The pressure drop due to acceleration of flow, Δp_{ac} (Pa), is defined as:

$$\Delta p_{ac} = \left(\rho_{out}\ u_{out}^2 - \rho_{in}\ u_{in}^2\right) = G^2\left(\frac{1}{\rho_{out}} - \frac{1}{\rho_{in}}\right). \qquad (7)$$

The pressure drop due to gravity, Δp_g (Pa), is defined as:

$$\Delta p_g = \pm g\left(\frac{\rho_{out} + \rho_{in}}{2}\right) L \sin\theta\,, \qquad (8)$$

where θ is the test-section inclination angle to the horizontal plane, sign "+" is for the upward flow and sign "–" is for the downward flow.

The pressure drop due to gravity, Δp_g, at supercritical pressures can be obtained through:

$$\Delta p_g = \pm g\left(\frac{H_{out}\ \rho_{out} + H_{in}\ \rho_{in}}{H_{out} + H_{in}}\right) L \sin\theta\,. \qquad (9)$$

CONCLUSIONS

1. Electrical-power generation is the key factor for advances in industry, agriculture, technology and the level of living. Also, strong power industry with diverse energy sources is very important for country independence.
2. In general, electrical energy can be generated from: 1) burning mined and refined energy sources such as coal (40%), natural gas (23%), oil (4%), and nuclear (11%); and 2) harnessing energy sources such as hydro (17%), and

biomass, wind, geothermal, solar, and wave power (all together about (5%).

3. Today, the main sources for electrical-energy generation are: 1) thermal power – primarily using coal and secondarily - natural gas; 2) "large" hydro power; and 3) nuclear power from various reactor designs. The balance of the energy sources is from using oil, biomass, wind, geothermal and solar, and have visible impact just in some countries.
4. The driving force in the power industry is thermal efficiency or just efficiency for some energy sources. Modern power plants have the following gross thermal efficiencies: Combined-cycle power plants up to 62%; supercritical-pressure thermal power plants – up to 55%; subcritical-pressure thermal power plants – up to 43%; carbon-dioxide-cooled and sodium-cooled reactors Nuclear Power Plants (NPPs) – up to 40 and 42%, respectively; and water-cooled reactors NPPs – 30–36% only.
5. According to the thermodynamics higher thermal efficiencies correspond to higher temperatures and pressures including supercritical ones. Therefore, new power cycles are being developed worldwide, which include supercritical-pressure Rankine "steam" cycle, supercritical-pressure Brayton gas cycle with working fluids such as helium, nitrogen-helium (80%/20%), carbon dioxide, etc. and various other combined cycles.

NOMENCLATURE

A area, m^2
c_p specific heat at constant pressure, J/kg K
$\bar{c}_p$ averaged specific heat within range ($T_w - T_b$); $\left(\frac{H_w - H_b}{T_w - T_b}\right)$, J/kg K
D inside diameter, m
D_{hy} hydraulic-equivalent diameter, m; $\left(\frac{4\,A_{fl}}{P_{wetted}}\right)$
G mass flux, kg/m^{2}s; $\left(\frac{m}{A_{fl}}\right)$
g gravitational acceleration, m/s^2
H specific enthalpy, J/kg
HTC heat transfer coefficient, W/m^{2}K
k thermal conductivity, W/m K
L length, m
m mass-flow rate, kg/s; $(\rho\,V)$
P, p pressure, Pa
Q heat-transfer rate, W
q heat flux, W/m^2; $\left(\frac{Q}{A_h}\right)$
s specific entropy, J/kg K
T, t temperature, °C or K
u axial velocity, m/s
V volumetric flow rate, m^3/s
W work, J

Greek Letters

α thermal diffusivity, m^2/s; $\left(\frac{k}{c_p\,\rho}\right)$
Δ difference
η efficiency
μ dynamic viscosity, Pa s
P_{wetted} wetted perimeter, m
ρ density, kg/m^3
υ kinematic viscosity, m^2/s
ξ friction coefficient

Non-Dimensional Numbers

Nu Nusselt number; $\left(\frac{HTC\,D}{k}\right)$
Pr Prandtl number; $\left(\frac{\mu\,c_p}{k}\right) = \left(\frac{\upsilon}{\alpha}\right)$
$\overline{\mathbf{Pr}}$ averaged Prandtl number within range ($T_w - T_b$); $\left(\frac{\mu\,\bar{c}_p}{k}\right)$
Re Reynolds number; $\left(\frac{G\,D}{\mu}\right)$

Symbols with an overbar denote average or mean values

Subscripts or Superscripts

ac acceleration
ave average
b bulk
comp compressor
cr critical
dht deteriorated heat transfer
el electrical
fl flow
fr friction
g gravitational
h heated
hy hydraulic
in inlet
out outlet or outside
p pressure
pc pseudocritical
sat saturation
th thermal
tot total
turb turbine
w wall

Acronyms and abbreviations widely used in text and list of references

AGR Advanced Gas-cooled Reactor
BN Fast Sodium (reactor) (in Russian abbreviations)
BWR Boiling Water Reactor
DHT Deteriorated Heat Transfer
EEC Electrical Energy Consumption
Eff. Efficiency
EU European Union
GFR Gas-cooled Fast Reactor
GIF Generation IV International Forum
HDI Human Development Index

HT	Heat Transfer
HTC	Heat Transfer Coefficient
HTR	High Temperature reactor
ID	Inside Diameter
IHT	Improved Heat Transfer
LFR	Lead-cooled Fast Reactor
LNG	Liquefied Natural Gas
MSR	Molten Salt Reactor
NHT	Normal Heat Transfer
NIST	National Institute of Standards and Technology (USA)
NPP	Nuclear Power Plant
OD	Outside Diameter
PWR	Pressurized Water Reactor
RBMK	Reactor of Large Capacity Channel type (in Russian abbreviations)
R&D	Research and Development
SCP	SuperCritical Pressure
SCW	SuperCritical Water
SCWR	SuperCritical Water-cooled Reactor
SFR	Sodium Fast Reactor
UK	United Kingdom
UN	United Nations
US or USA	United States of America
VHTR	Very High-Temperature Reactor

REFERENCES

[1] Handbook of Generation IV Nuclear Reactors, 2016. Editor: I.L. Pioro, Elsevier – Woodhead Publishing (WP), Duxford, UK, 940 pages.

[2] Pioro, I. and Duffey, R., 2015. Nuclear Power as a Basis for Future Electricity Generation, *ASME Journal of Nuclear Engineering and Radiation Science*, Vol. 1, No. 1, 19 pages. Free download: http://nuclearengineering.asmedigitalcollection.asme.org/article.aspx?articleID=2085849.

[3] Pioro, I. and Kirillov, P., 2013. Current Status of Electricity Generation at Thermal Power Plants, Chapter in the book: Materials and Processes for Energy: Communicating Current Research and Technological Developments, Energy Book Series #1, Editor: A. Méndez-Vilas, Publisher: Formatex Research Center, Spain, pp. 796-805. Free download: http://www.formatex.info/energymaterialsbook/book/796-805.pdf.

[4] Pioro, I. and Kirillov, P., 2013. Current Status of Electricity Generation at Nuclear Power Plants, Chapter in the book: Materials and Processes for Energy: Communicating Current Research and Technological Developments, Energy Book Series #1, Editor: A. Méndez-Vilas, Publisher: Formatex Research Center, Spain, pp. 806-817. Free download: http://www.formatex.info/energymaterialsbook/book/806-817.pdf.

[5] Dragunov, A., Saltanov, Eu., Pioro, I., Kirillov, P., and Duffey, R., 2015. Power Cycles of Generation III and III^+ Nuclear Power Plants, ASME Journal of Nuclear Engineering and Radiation Science, Vol. 1, No. 2, 10 pages.

[6] Pioro, I. and Kirillov, P., 2013. Generation IV Nuclear Reactors as a Basis for Future Electricity Production in the World, Chapter in the book: Materials and Processes for Energy: Communicating Current Research and Technological Developments, Energy Book Series #1, Editor: A. Méndez-Vilas, Publisher: Formatex Research Center, Spain, pp. 818-830. Free download: http://www.formatex.info/energymaterialsbook/book/818-830.pdf.

[7] NIST (National Institute of Standards and Technology), 2013. NIST Standard Reference Database 23. NIST Reference Fluid Thermodynamic and Transport Properties - REFPROP. Ver. 9.1. Technology Administration, U.S. Department of Commerce: http://www.nist.gov/srd/nist23.cfm.

[8] Pioro, I., Mahdi, M., and Popov, R., 2017. Application of Supercritical Fluids in Power Engineering, Chapter 13 in book: Advanced Applications of Supercritical Fluids in Energy Systems, Editors: L. Chen and Yu. Iwamoto, IGI Global, Hershey, PA, USA, 626 pages.

[9] Pioro, I. and Mokry, S., 2011. Thermophysical Properties at Critical and Supercritical Conditions, Chapter in book "Heat Transfer. Theoretical Analysis, Experimental Investigations and Industrial Systems", Editor: A. Belmiloudi, INTECH, Rijeka, Croatia, pp. 573-592. Free download: http://www.intechopen.com/books/heat-transfer-theoretical-analysis-experimental-investigations-and-industrial-systems/thermophysical-properties-at-critical-and-supercritical-pressures.

[10] Pioro, I.L. and Duffey, R.B., 2007. Heat Transfer and Hydraulic Resistance at Supercritical Pressures in Power Engineering Applications, ASME Press, New York, NY, USA, 334 pages.

[11] Mokry, S., Pioro, I.L., Farah, A., King, K., Gupta, S., Peiman, W. and Kirillov, P., 2011. Development of Supercritical Water Heat-Transfer Correlation for Vertical Bare Tubes, *Nuclear Engineering and Design*, Vol. 241, pp. 1126-1136.

[12] Pioro, I. and Mokry, S., 2011. Heat Transfer to Fluids at Supercritical Pressures, Chapter in book "Heat Transfer. Theoretical Analysis, Experimental Investigations and Industrial Systems", Editor: A. Belmiloudi, INTECH, Rijeka, Croatia, pp. 481-504. Free download: http://www.intechopen.com/books/heat-transfer-theoretical-analysis-experimental-investigations-and-industrial-systems/heat-transfer-to-supercritical-fluids.

[13] Pioro, I., Duffey, R. and Dumouchel, T., 2004. Hydraulic Resistance of Fluids Flowing in Channels at Supercritical Pressures (Survey), Nuclear Engineering and Design, Vol. 231, No. 2, pp. 187–197.